Optical Engineering 47(1), 017006 (January 2008)

Image restoration of an off-axis three-mirror anastigmatic optical system with wavefront coding technology

Feng Yan
Chinese Academy of Science
Changchun Institute of Optics, Fine Mechanics and Physics
Optical Technology Research Center
Changchun 130033, China
and
Chinese Academy of Science
Graduate School
Beijing 100084, China

Li-gong Zheng
Xue-jun Zhang
Chinese Academy of Science
Changchun Institute of Optics, Fine Mechanics and Physics
Optical Technology Research Center
Changchun 130033, China

Abstract. Wavefront coding technology can extend the depth of focus of a well-corrected three-mirror anastigmatic optical system by about ten times, but the image obtained directly by charge-coupled devices blurs at the same time. An effective image restoration must be applied to these blurred images. This paper describes an innovative method that restores the blurred image, which combines the optical design software and mathematical software. The point spread function of system with wavefront coding technology is quite different from the usual and difficult to simulate by a disk function or other simple function in most cases. The commercial optical design software is applied to obtain the point spread function. If a 1×1-pixel image with brightness 255 is set as the point source of a optical system, the result of calculation software using a ray tracing algorithm will itself be the digital point spread function. This is proven to be a simple and effective way to acquire the complicated point spread functions of unusual optical systems such as those using wavefront coding technology. A regularization factor and contrast-adjusting factors are introduced into the classical Wiener filter, which achieves good restored images: the root-mean-square error is less than 0.0193, while the peak signal-noise ratio is higher than 23.7. Some parameters of the filter can be adjusted so that the restored image is more suitable for evaluation by eye. It is also shown that a single filter can restore all the images within the extended depth of focus. [DOI: 10.1117/1.2835687]

Subject terms: wavefront coding; PSF; Wiener filtering; regularization; contrast; noise.

Paper 070439RR received May 23, 2007; revised manuscript received Aug. 23, 2007; accepted for publication Aug. 27, 2007; published online Jan. 31, 2008.

1 Introduction

It is difficult to maintain the focal plane position of a spaceborne optical system, due to temperature fluctuation in the space environment as well as launch shock. Most spaceborne optical systems employ refocusing mechanisms to overcome this problem. There are three main disadvantages associated with these devices: first, they are hard to fabricate, which increases the manufacturing cost of the system; second, they are quite complicated, which makes the system more unsteady and more sensitive to working condition; and third, they cannot work well unless the exact magnitude of misfocus is known, which is difficult to measure. The relative aperture of spaceborne infrared cameras is often designed extraordinarily large so as to collect as much power as possible. But according to the formula DOF $=2\lambda(\text{f number})^2$, the depth of focus is inversely proportional to the square of the relative aperture. But large depth of focus and large relative aperture cannot be obtained at the same time. In most infrared system the depth of focus is extremely short, which complicates alignment and misfocus compensation.

An innovative technique called wavefront coding provides a new way to extend the depth of focus and to control misfocus aberration and misfocus-related aberrations (including astigmatism, Petzval curvature, and temperature-related and alignment-related misfocus) of spaceborne digital imaging systems.[1–4] The essential idea of this technology is to append a phase distribution, based on the theory of ambiguity functions to the pupil function of a well-corrected optical system by means of phase masking, surface modulation, and so on. If the image plane is moved apart from its original position to either side, a blurred image will be obtained because of the changed pupil function, but the image will remain nearly the same, in spite of the different image distance, over a range of several times the depth of focus. The degree of blurring of images in this range is quite insensitive to misfocus aberration, an effect that can be regarded as an extension of the depth of focus. Because the blurring of all images in the extended depth of focus is nearly the same, and the additive phase distribution is well known, all these intermediate images can be restored to sharp and clear ones by a simple filtering process. The digital imaging processing of images of this kind is discussed in this paper.

There are a huge number of papers on image restoration using different techniques, such as Fourier transform, wavelet transform, adaptive filter, nonlinear filter, morpho-

0091-3286/2008/$25.00 © 2008 SPIE

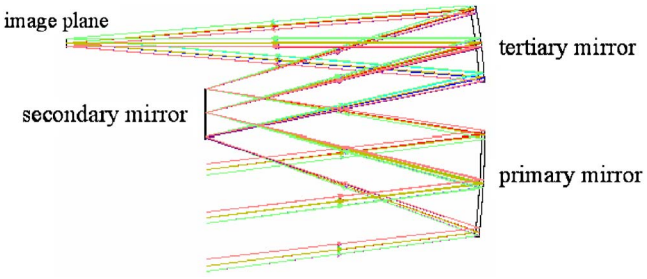

Fig. 1 Layout of the original TMA system.

logical operator, and so on. Since image restoration is a typical inverse problem, the Tikhonov regularization method, which prevents instability of solutions with respect to the noise of the original data and ensures global convergence, has been proven to be very powerful. The time and computational cost can be greatly reduced if a good regularization parameter is selected.[5–7] Yap and Guan[8] proposed a new approach to adaptive image regularization based on a neural network (hierarchical cluster model), which is superior in suppressing noise and ringing in the smooth background while effectively preserving the fine details in the texture and edge regions. Hong et al.[9,10] introduced a regularized mixed-norm function combined with the least mean square (LMS) and the least mean fourth (LMF) functions as well as a smoothing function for dealing with various kinds of noise the absence of knowledge of the noise. Demaret et al.[11] presented a heuristic algorithm for the choice of a wedgelet regularization parameter for the purpose of denoising in the case where the noise variance σ^2 is not known. Mastronardi et al.[12] studied the ill-posed blind deconvolution problems encountered in image deblurring when both the image and the blurring function are uncertain and proved that regularized structured total least-squares algorithms improve the computational efficiency.

Research on restoration of images by wavefront-coded systems has also been carried out. Bradbum et al.[13] introduced the traditional least-squares method. Based on their work, van der Gracht et al.[14] proposed the modified residual-norm steepest descent (MRNSD) method and obtained excellent results. The regularization method and some postprocessing are demonstrated in this paper.

Table 1 Main parameters of the investigated TMA optical system

Focus	1650 mm
f number	6
Field of view	1.5×5 deg
Working wavelength	0.5 μm

2 Working Fundamentals

Previous research has led to the well-corrected three-mirror anastigmatic (TMA) system (parameters in Table 1) shown in Fig. 1. The primary mirror and the tertiary mirror of the original system are both hyperboloids and of rectangular aperture, while the secondary mirror is a standard paraboloid of circular aperture, whose surface can be expressed as

$$z(x,y) = \frac{c(x^2+y^2)}{1+[1-(1+k)c^2(x^2+y^2)]^{1/2}}, \tag{1}$$

where k is the conic constant and $c=1/r$, where r is the radius of curvature.

The depth of focus of this system can be extended about tenfold by making a small change in the surface of the secondary mirror according to wavefront coding technology. An extra term is appended to the surface sag while k and c remain the same:

$$z(x,y) = \frac{c(x^2+y^2)}{1+\sqrt{1-(1+k)c^2(x^2+y^2)}} + \beta(x^3+y^3) \tag{2}$$

where

$$\beta = \varepsilon \cdot \frac{\lambda}{2\pi} \cdot \frac{R_{\text{stop}}}{R_{\text{EP}}} \cdot \frac{1}{R_{\text{stop}}^3}, \tag{3}$$

in which $1/R_{\text{stop}}^3$ is a normalization factor, and $\varepsilon \gg 20$.

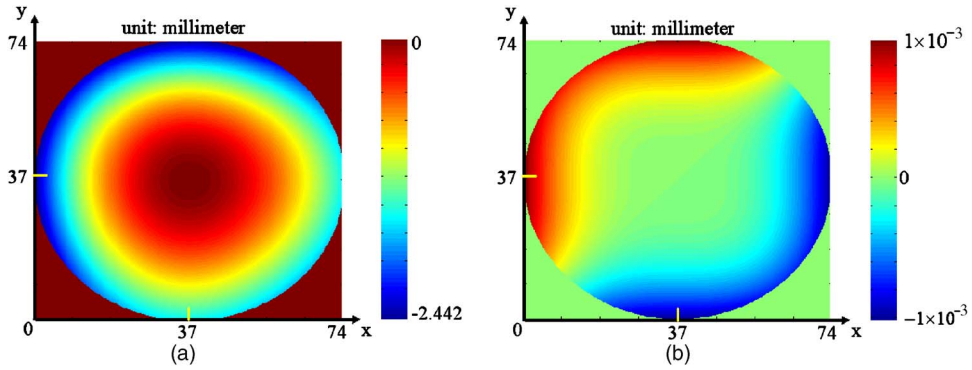

Fig. 2 (a) Surface of the redesigned secondary mirror of the new system. (b) Difference in sag of the secondary mirror between the new system and the original system. Here (a) is exaggerated by magnifying the additive term $\beta(x^3+y^3)$ for better observation, since the actual value of $\beta(x^3+y^3)$ is so small that the surface transformation due to this term can hardly be noticed by the eye.

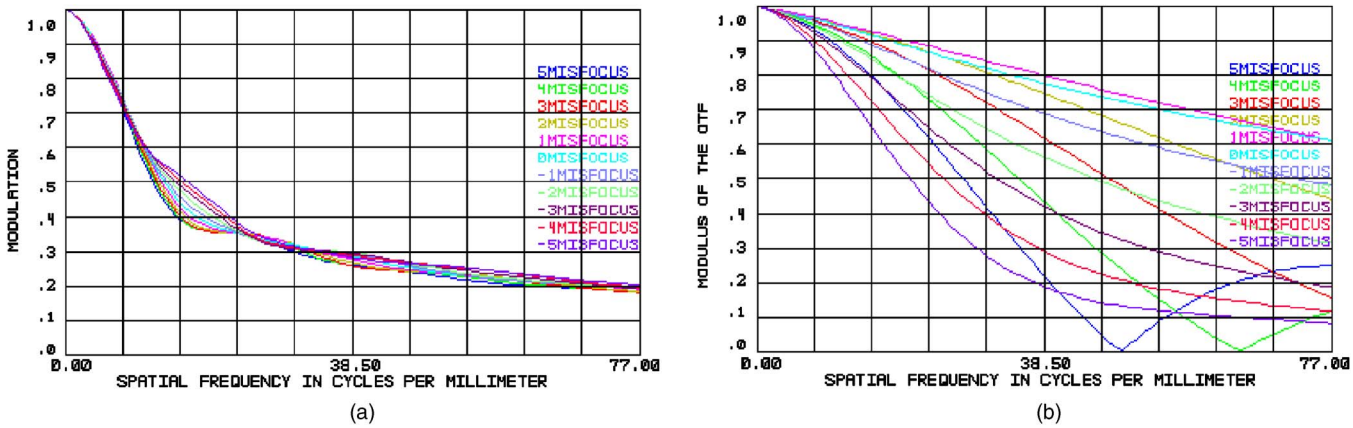

(a) (b)

Fig. 3 Comparison of MTF curves between (a) the new system and (b) the original system on 11 equally spaced image planes.

The surface of the secondary mirror after transforming has a particular profile shown in Fig. 2. In the following the system with extended depth of focus is called the *new system* to distinguish it from the original system.

In Eq. (3) ε can be regarded as an extension factor of the depth of focus. The extended depth of focus is proportional to ε, while the MTF—especially its high-frequency part—will drop when ε increases. Too large ε is not acceptable, for the high-frequency part of the MTF will drop so much that it is more difficult to realize restoration, although the depth of focus can be extended greatly in that case. It is important to set a proper value of ε to make a reasonable trade-off between extended depth of focus and magnitude of MTF. Also, ε has to be much larger than 20, since only when this requirement is satisfied can the MTF be kept the nearly the same over a larger range than the original depth of focus, according to the theory of the ambiguity function (AF), which is fundamental to wavefront coding technology.[15,16]

Suppose the back focal length of the original system is D and the depth of focus is DOF. For the new system 11 equally spaced image planes from $D-5$ DOF to D +5 DOF can be selected, and the MTFs of both new system and original system on each image plane can be calculated. As shown in Fig. 3, the MTF curves of the new system remain nearly the same regardless of the image plane distance, while those curves of the original system differ distinctly from each other.

It can be shown from the high similarity of MTF curves that the intermediate images in the extended depth of focus must be nearly the same, although they are blurred. The restoration of these intermediate images is discussed in the next section.

3 Calculation of Point Spread Function

For a given optical system, the image formation can be expressed as

$$g(x,y) = \mathrm{psf}(x,y) \ ** \ f(x,y) + n(x,y),$$

where $\mathrm{psf}(x,y)$ is the point spread function (PSF), $f(x,y)$ is the target function, $n(x,y)$ is the noise level, $g(x,y)$ represents the degraded image, and $**$ is the convolution operator. The universal digital filtering process for image restoration can be written as follows:[17]

$$\hat{F}(u,v) = \left[\frac{H^*(u,v)}{|H(u,v)|^2}\right]^{\alpha} \times \left[\frac{H^*(u,v)}{|H(u,v)|^2 + \gamma P_n(u,v)/P_f(u,v)}\right]^{1-\alpha} G(u,v), \quad (4)$$

where $G(u,v)=F\{g(x,y)\}$, $H(u,v)=F\{\mathrm{psf}(x,y)\}$, P_n is the noise power spectrum, and α and γ are parameters, of which α is selected between 0 and 1 and γ is a positive constant depending on the situation.

Obviously, if the exact magnitudes of $\mathrm{psf}(x,y)$ and $n(x,y)$ are known, image restoration will be easily realized. In most cases of image blurring by misfocus aberration, $\mathrm{psf}(x,y)$ is simulated by a disk function, whose Fourier transform is a Bessel function. Related research has shown that images whose PSF is a Gaussian can be restored well in this condition. But the PSF of a system with wavefront coding technology is far from Gaussian, as shown in Fig. 4. Compared to original system's, the energy of new system's PSF extends over a much wider space. Furthermore, the normalized pupil function of the new system in one dimension is[16]

$$\mathrm{Pupil}(x) = \begin{cases} \dfrac{1}{\sqrt{2}} \exp(j\varepsilon x^3) & \text{for } |x| \le 1, \\ 0 & \text{otherwise}, \end{cases} \quad (5)$$

where ε is the same as in Eq. (3). The Fourier transform of Eq. (5) is the analytical form of the PSF of the new system, which is a Bessel function of the second kind:

$$Psf(x) = \frac{2}{3}(-\varepsilon)^{1/3} \sqrt{\frac{x}{(-\varepsilon)^{1/3}}} J_k\left(\frac{1}{3}, \frac{2}{9}\sqrt{3}\left(\sqrt{\frac{x}{(-\varepsilon)^{1/3}}}\right)^{3/2}\right). \quad (6)$$

The usual method of restoring images with a Gaussian PSF will not work well, for the PSF of the new system is quite different from Gaussian and difficult to approximate exactly by simple functions such as the disk function. For-

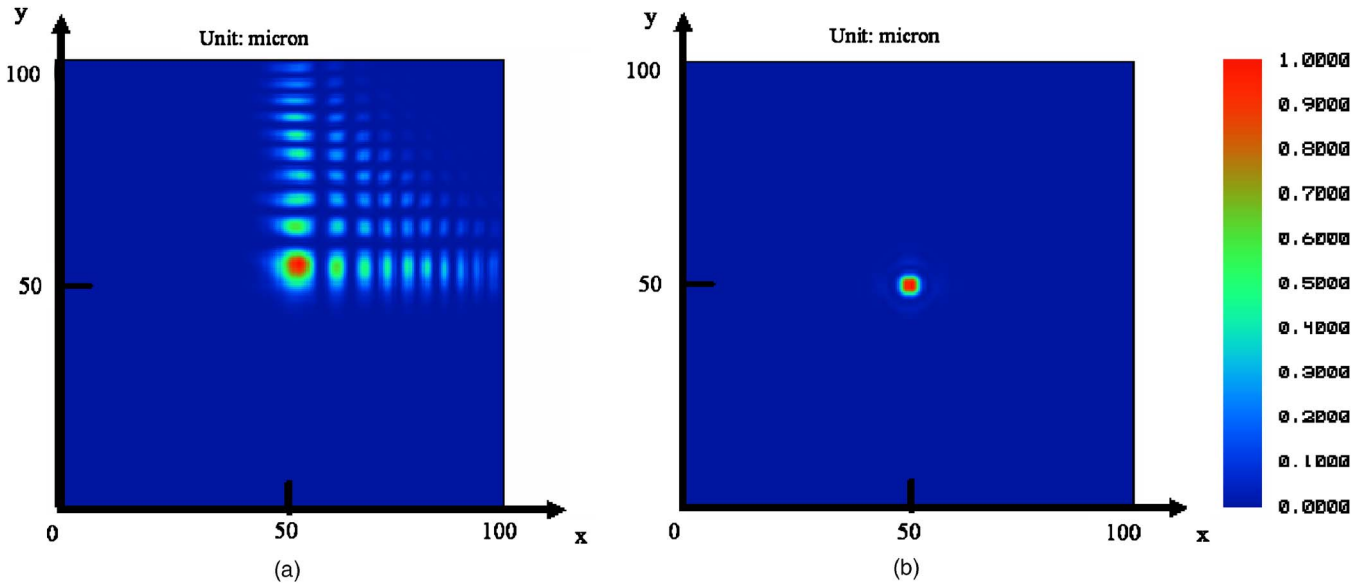

Fig. 4 Comparison of PSF between (a) the new system and (b) the original system.

tunately, because all characteristics of the new system are known exactly, it is possible to determine the PSF experimentally. In fact, that is a traditional way. McGlamery successfully restored telescopic images blurred by atmospheric turbulence through a PSF obtained by experiment in the early 1960s.[17] Today the same work can be performed by computer simulation instead of setting up the actual optical system.

First, a 1×1-pixel digital image is constructed and its brightness set to 255. This one-pixel image can be regarded as a point source. Secondly this spot source is shot by the new system by means of optical design software through a strict ray tracing algorithm. The image plane is set at 400×400 pixels, and each pixel is set 6.85×6.85 μm. Altogether 1.5×10^7 rays are traced. An image of a spot is obtained on the image plane, which can be taken as the PSF of the system. Therefore all the residual design error and added pupil aberration is comprised in the PSF.

It can be observed from Fig. 5 that the PSF of the new system is very complex. A 21×21 region is extracted for the next procedure.

4 Image Restoration

A bar target (Fig. 6) was set as the target image and calculated by the new system, using the same method as for the PSF calculation. All conditions are the same except the y field and number of rays. The degraded image is presented in Fig. 7.

A Wiener filter is considered to be an efficient technique in image restoration. If α is set to zero, then Eq. (4) takes on the typical form of Wiener filter as follows:

$$\hat{F}(u,v)=\frac{1}{H(u,v)}\frac{|H(u,v)|^2}{|H(u,v)|^2+\gamma P_n(u,v)/P_f(u,v)}G(u,v),$$

$$H^*(u,v)=\frac{|H(u,v)|^2}{H(u,v)}. \tag{7}$$

Furthermore, the regularization factor is introduced into the

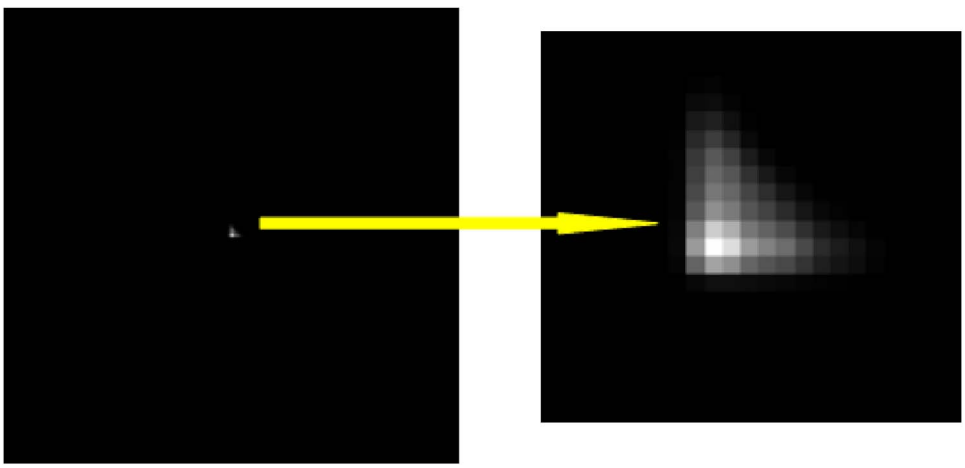

Fig. 5 Sampling PSF of new system for image restoration.

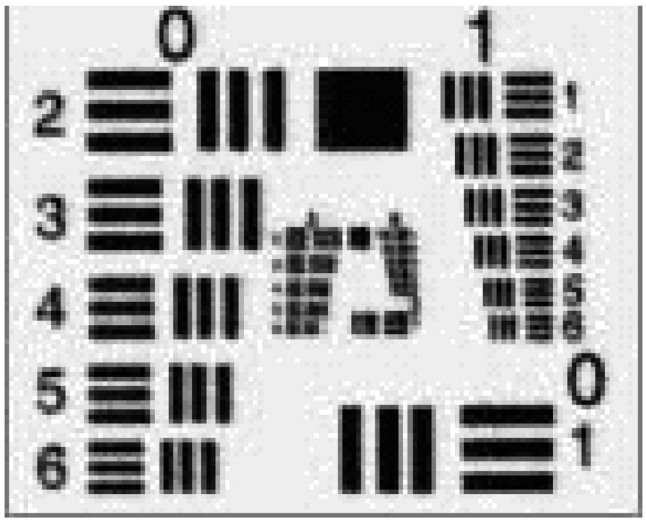

Fig. 6 Target image.

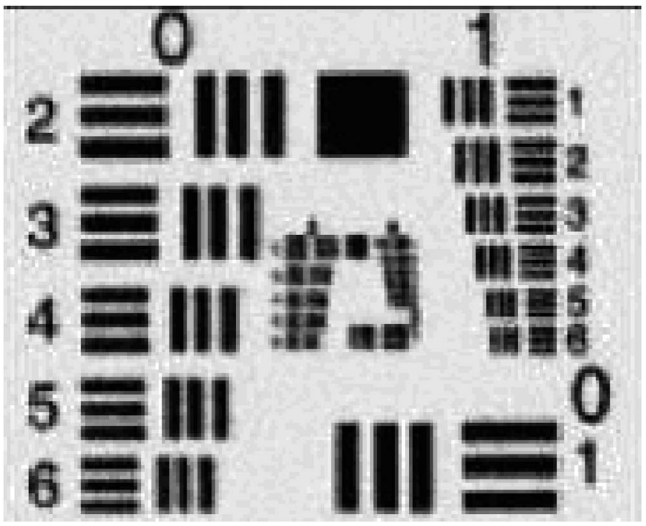

Fig. 8 Ideal image produced by original system.

filter, which makes the solution more stable and faster convergent according to Tikhonov's theory.[5–7,18] Then the restored process can be expressed as follow:

$$\hat{F}(u,v) = \frac{1}{H(u,v)} \frac{\alpha_1 |H(u,v)|^2}{\alpha_2 |H(u,v)|^2 + \beta \mathbf{L}_1^T \mathbf{L}_1 + \gamma} G(u,v), \tag{8}$$

where α_1 and α_2 are contrast-adjusting factors, β is a regularization factor, $\mathbf{L}_1$ is the Fourier transform of the Laplacian operator, γ is a positive constant.

MATLAB software is used to process the image restoration. The first step is to input the extract from the PSF and perform Fourier transformation to generate the transfer function H. The four parameters α_1, α_2, β, γ can be determined by iterative processing. Different constants lead to different restorations. An ideal image (Fig. 8) obtained by a traditional well-corrected system in the same condition is introduced for comparison and judging the quality of the restored image. Figure 9(a) is the restored image with optimum factors, while Fig. 9(b) is restored by the traditional Wiener filter. According to the theory of wavefront coding technology, the depth of focus is extended at the cost of not only degraded image quality but also lower signal-noise ratio. It can be supposed that noise is magnified in the imaging process. The digital filter cannot manage reducing the noise to normal level, so there is some residual noise in the image.

The root-mean-square error (RMSE) is taken as the criterion to estimate the quality of the restored image. The RMSE of Fig. 9(a) with respect to Fig. 8 is less than 0.0193; its peak signal-noise ratio (PSNR) is higher than 23.7, while the PSNR of Fig. 9(b) is about 21.64. The edge of the restored image can be extracted by a Laplacian-Gaussian operator, as Fig. 10 shows. It can be seen that the edges can be well recognized by the computer, which proves our restoration is effective. From the comparison of histograms of Fig. 8 and Fig. 9(a) in Fig. 11, it can be observed that the gray-level distribution of the restored image agrees with the standard one very well.

But when the restored images are evaluated by eye, the RMSE rule is not the best criterion for estimating image quality, because it weights all errors equally, whereas human vision has more tolerance to errors in the dark parts and fringes of an image. So the images restored according to the RMSE criterion are not always suitable for

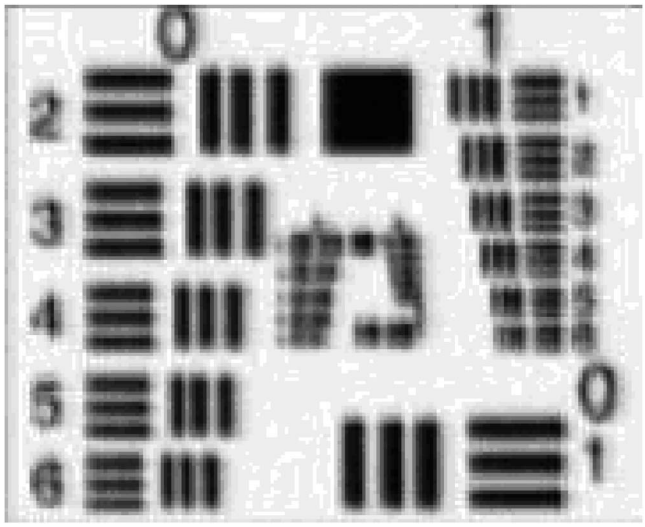

Fig. 7 Blurred image.

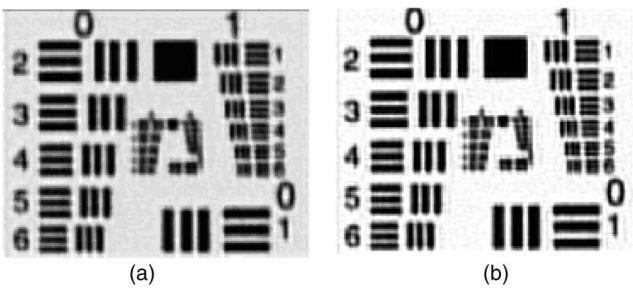

(a) (b)

Fig. 9 Image restored by (a) the filter presented in this paper, (b) a typical Wiener filter.

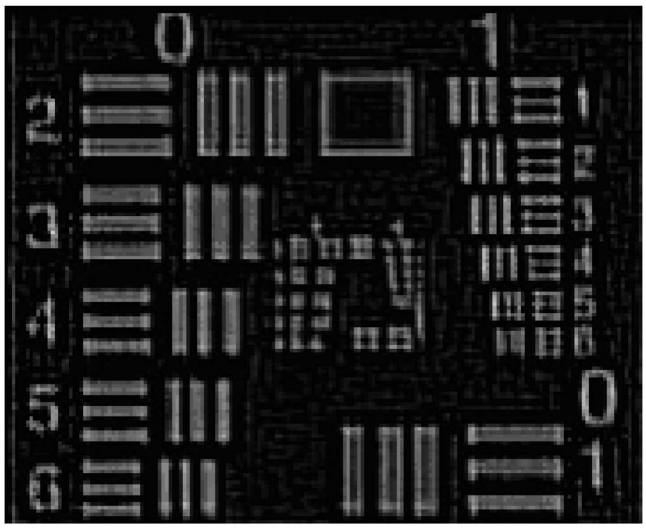

Fig. 10 Outline of the restored image in Fig. 9(a).

viewing.[17,19] There are two methods to make some improvement: One is to use a standard Wiener filter, with the regularization factor β set to zero and other parameters selected again, in which case contrast enhancement is needed; the other is to use the same filter but adjust the factors (especially, increase γ). The results are shown in Fig. 12. Although RMSE of the two images in Fig. 12 is larger than that of the standard, these image are actually more suited to human vision.

These two kinds of images can be used for different application. The former has adequate gray levels and preserves the most information of target image, so it is fit for large-scale ordinary observation. The latter improves the contrast between object and background and gives more detail of the object, so it is better suited for observation of a particular small area.

5 Image Restoration with Extended Depth of Focus

It has been indicated before that the image quality remains almost the same with the extended depth of focus and can be restored by a single digital filtering process. The MTF curves of 11 image planes with DOF of order 10 are presented in Fig. 3(a); the intermediate images and restored results of these 11 image planes are shown in Fig. 13. The parameters of the digital filter are set so that the restored images are fit for eye evaluation, and those same parameters are used for all the 11 images.

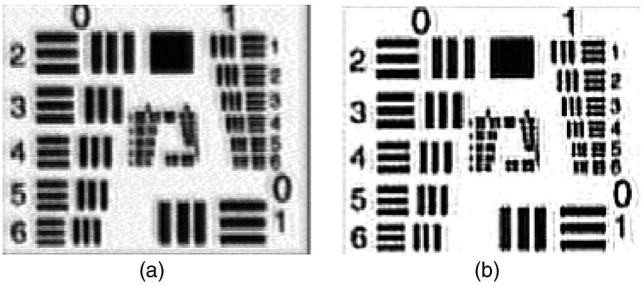

(a) (b)

Fig. 12 (a) Image restored by typical Wiener filter. (b) Image restored by improved primary filter.

6 Conclusion

Restoration of images by a wavefront-coded TMA system has been presented in this paper. It is shown in Sec. 2 that the PSF of the new system is quite different from Gaussian, so that it is difficult to fit with a simple function, and its analytical form is complicated, so that it will cost much calculation and time for further restoration. This paper proposes a simple and efficient method to calculate the PSF of the new system. A discrete PSF for digital filtering can be obtained directly in a short time by means of a ray tracing algorithm, which is easy to realize in optical design software.

In the image restoration, a regularization factor and contrast-adjusting factors are introduced into the classical Wiener filter. The PSNR of the image restored by the improved Wiener filter is about 2 dB higher than that of the image restored by the traditional Wiener filter. It is shown that the restored image can be made more suitable for the eye by means of adjusting some parameters of the filter. It is also proven that images with extended depth of focus can be restored by a single filter, which confirms the possibility of reliable image encoding.

There are still some confusing problems to solve in future work. For one thing, the target image used here is very

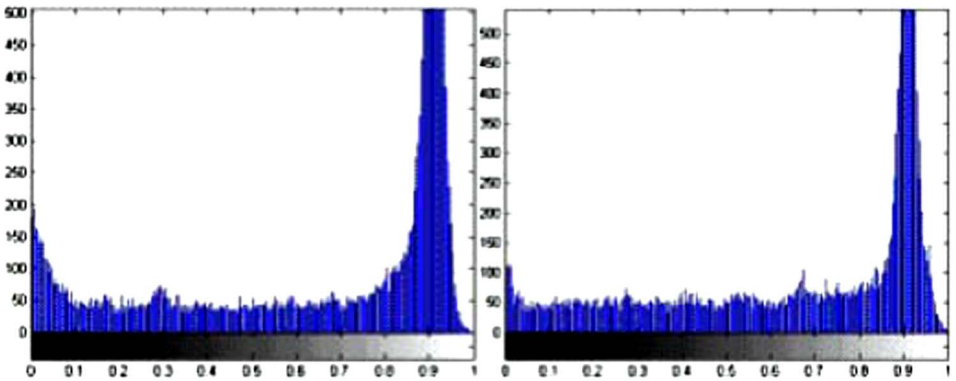

Fig. 11 Comparison of histograms between ideal image (left) and restored image (right).

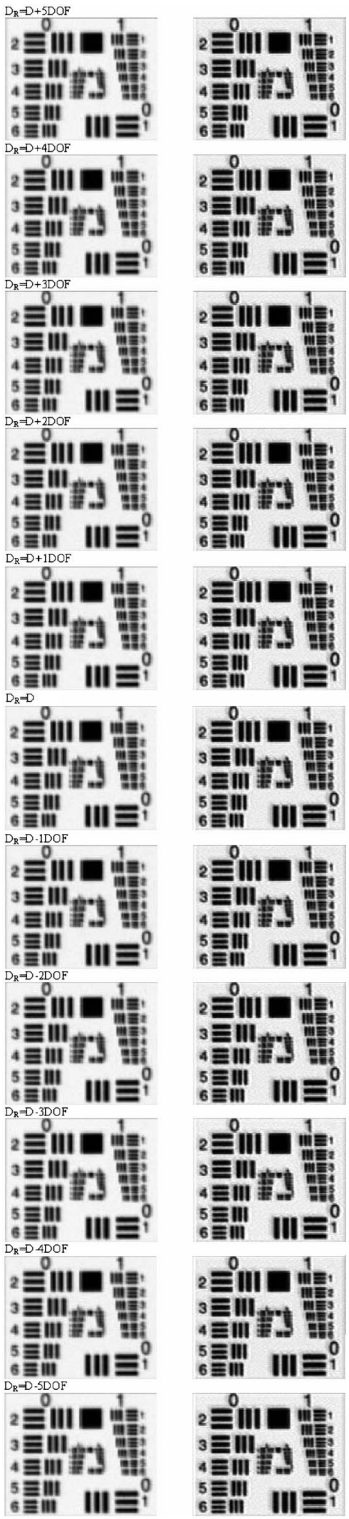

Fig. 13 Comparison of original images (left) and restored images (right).

simple: the background is uniform, the object is compact, and the contrast between them is very sharp. The ability of the filter in this paper to restore more complex images needs to be tested, but some improvement is expected. For another thing, effort should be made to reduce the residual noise in the restored images. More joint optimization of both optical design and digital image processing is necessary to obtain sharper restored images.

Acknowledgment

This research is sponsored by National Fund of Outstanding Talent, No. 69925512.

References

1. E. R. Dowski, Jr., R. H. Cormack, and S. D. Sarama, "Wavefront coding: jointly optimized optical and digital imaging systems," *Proc. SPIE* **4041**, 114–120 (2000).
2. E. R. Dowski, Jr. and K. S. Kubala, "Modeling of wavefront coded imaging systems," *Proc. SPIE* **4736**, 116–126 (2002).
3. E. R. Dowski, Jr. and G. E. Johnson, "Wavefront coding: a modern method of achieving high performance and/or low cost imaging systems," *Proc. SPIE* **3779**, 137–145 (1999).
4. K. Kubala, E. Dowski, J. Kobus, and B. Brown, "Design and optimization of aberration and error invariant space telescope systems," *Proc. SPIE* **5524**, 54–65 (2004).
5. J. Xie and J. Zou, "An improved model function method for choosing regularization parameters in linear inverse problems," *Inverse Probl.* **18**, 641–643 (2002).
6. G. H. Golub, P. C. Hansen, and D. P. O'Leary, "Tikhonov regularization and total least squares," *SIAM J. Matrix Anal. Appl.* **21**, 185–194 (1999).
7. G. Landi and F. Zama, "The active-set method for nonnegative regularization of linear ill-posed problems," *Appl. Math. Comput.* **175**, 715–729 (2006).
8. K. H. Yap and L. Guan, "Adaptive image restoration based on hierarchical neural networks," *Opt. Eng.* **39**(7), 1877–1890 (2000).
9. M.-C. Hong, T. Stathaki, and A. K. Katsaggelos, "Iterative regularized least-mean mixed-norm image restoration," *Opt. Eng.* **41**(10), 2515–2524 (2002).
10. M.-C. Hong, T. Stathaki, and A. K. Katsaggelos, "Iterative regularized mixed norm multichannel image restoration," *J. Electron. Imaging* **14**(1), 013004-1–013004-9 (2005)
11. L. Demaret, F. Friedrich, H. Führ, and T. Szygowski, "Multiscale wedgelet denoising algorithms," *Proc. SPIE* **5914**, 59140X-1–59140X-12 (2005).
12. N. Mastronardi, P. Lemmerling, A. Kalsi, D. P. O'Leary, and S. Van Huffel, "Implementation of the regularized structured total least squares algorithms for blind image deblurring," *Linear Algebr. Appl.* **391**, 203–221 (2004).
13. S. Bradbum, W. T. Cathey, and E. R. Dowski, "Realizations of focus invariance in optical-digital systems with wave-front coding," *Appl. Opt.* **36**(35), 9157–9166 (1997).
14. J. van der Gracht, J. G. Nagy, V. P. Pauca, and R. J. Plemmons, "Iterative restoration of wavefront coded imagery for focus invariance," *Appl. Opt.* **36**, 9157–9166 (1997).
15. A. R. FitzGerrell, E. R. Dowski, Jr., and W. T. Cathey, "Defocus transfer function for circularly symmetric pupils," *Appl. Opt.* **36**(23), 5796–5804 (1997).
16. E. R. Dowski, Jr. and W. T. Cathey, "Extended depth of field through wave-front coding," *Appl. Opt.* **34**(11), 1859–1866 (1995).
17. K. R. Castleman, *Digital Image Processing* (in Chinese), Publishing House of Electronics Industry, Beijing (2004).
18. J. W. Wang and Y. Cao, *Graphics and Image Processing with Matlab6.5.* (in Chinese), National Defense Industry Publishing House, Beijing (2005).
19. M. Petrou and P. Bosdogianni, *The fundamentals of Image Processing* (in Chinese), China Machine Press, Beijing (2005).

Feng Yan obtained his BS degree in physics (optics) in 2004 from Nankai University. After two years of study at Changchun Institute of Optics, Fine Mechanics and Physics, China Academy of Science, he is now a PhD candidate concentrating on wavefront coding technology, optical manufacturing, and testing.

Li-gong Zheng received his BE in engineering in 1992, and his PhD in optical engineering in 2003. Now he is working as an assistant professor at the Optical Technology Research Center, Changchun Institute of Optics, Fine Mechanics and Physics. His research interests include CCOS, aspherical surface fabrication and testing, and electronic engineering.

Xue-jun Zhang received his MS in engineering in 1993, and his PhD in optics in 1997. Now he is working as a professor at the Optical Technology Research Center, Changchun Institute of Optics, Fine Mechanics and Physics. His research interests include ultraprecision manufacturing, aspherical surface fabrication and testing, new optical materials and fabrication techniques, and computer applications.